ARMY RESEARCH LABORATORY

Controlled Deposition and Collection of Electro-spun Poly(ethylene oxide) Fibers

Joseph M. Deitzel
James D. Kleinmeyer
James K. Hirvonen
Nora C. Beck Tan

ARL-TR-2415 MARCH 2001

20010427 059

Approved for public release; distribution is unlimited.

Student's Quick Field™ is a trademark of Tera Analysis Company.

Teflon® is a registered trademark of E.I. DuPont de Nemours & Co., Inc.

The findings in this report are not to be construed as an official Department of the Army position unless so designated by other authorized documents.

Citation of manufacturer's or trade names does not constitute an official endorsement or approval of the use thereof.

Destroy this report when it is no longer needed. Do not return it to the originator.

Army Research Laboratory
Aberdeen Proving Ground, MD 21005-5066

ARL-TR-2415 March 2001

Controlled Deposition and Collection of Electro-spun Poly(ethylene oxide) Fibers

Joseph M. Deitzel
James K. Hirvonen
Nora C. Beck Tan
Weapons & Materials Research Directorate, ARL

James D. Kleinmeyer
XioTech, a Seagate Company

Approved for public release; distribution is unlimited.

Abstract

Electro-spinning is a process by which sub-micron polymer fibers can be produced with an electrostatically driven jet of polymer solution (or polymer melt). Electro-spun fibers are typically collected in the form of non-woven mats, which are of interest for a variety of applications, including semi-permeable membranes, filters, composite reinforcement, and scaffolding used in tissue engineering. A characteristic feature of the electro-spinning process is the onset of a chaotic oscillation of the electro-spinning jet. The current work demonstrates the feasibility of dampening this instability and controlling the deposition of sub-micron polymer fibers (<300 nm in diameter) on a substrate through use of an electrostatic lens element and collection target of opposite polarity. Real-time observations of the electro-spinning process have been made with high speed, high magnification imaging techniques. Fiber mats and yarns electro-spun from polyethylene oxide have been analyzed by wide angle electron diffraction optical microscopy and environmental electron microscopy.

ACKNOWLEDGMENTS

The authors would like to thank Professor Dan Marble from Tarleton State University, Stephensville, Texas, for his insightful comments with respect to ion beam optics, and Dr. Mike Mcquaide of the U.S. Army Research Laboratory for advice pertaining to high speed imagining. We would like to thank the American Society of Engineering Education and the Oak Ridge Institute for Science and Education, Tennessee, for their support of this work.

INTENTIONALLY LEFT BLANK

Contents

1. **Introduction** 1
2. **Experimental** 4
3. **Theory** 4
4. **Results and Discussion** 6
5. **Conclusion** 12

References 15

Distribution List 17

Report Documentation Page 19

Figures

1. Standard Electro-spinning Apparatus 2
2. Field Lines Calculated for a Syringe and Grounded Target Geometry 3
3. High Speed Image of Electro-spinning Process 3
4. Forces Exerted on a Charge Element by Neighboring Charge Elements 6
5. Multiple Field Electro-spinning Apparatus 7
6. Field Lines Calculated for Multiple Field Electro-spinning Geometry . 8
7. Image of Electro-spinning Jet 4 inches Below Capillary Orifice 9
8. Fibers Electro-spun From 10% Solution Concentration of PEO in Water 10
9. Electron Micrograph of PEO Fibers Electro-spun With Multiple Field Method 10
10. Electro-spun Fibers Collected on a Rotating Drum With the Multiple Field Electro-spinning Method 11
11. 2D WAXD Pattern Obtained From PEO Electro-spun Yarns 12
12. Plot of the Integrated Scattering Intensity as a Function of 2θ From Figure 11b 13
13. Powder WAXD Pattern for PEO Powder 13

INTENTIONALLY LEFT BLANK

CONTROLLED DEPOSITION AND COLLECTION OF ELECTRO-SPUN POLY(ETHYLENE OXIDE) FIBERS

1. Introduction

For almost 100 [1] years, it has been known that polymer fibers can be generated from an electrostatically driven jet of polymer solution (or polymer melt). This process, known as electro-spinning, has received much attention in the last decade because of its ability to consistently generate polymer fibers that range from 5 to 500 nanometers in diameter. Because of the small pore size and high surface area inherent in electro-spun textiles [2,3,4], these fabrics show promise for exploitation in soldier protective clothing and filtration applications [5]. Other exciting applications that are being explored include scaffolding for tissue growth [6], optical and electronic applications [7,8].

The schematic for a typical electro-spinning apparatus is depicted in Figure 1 and its associated field lines in Figure 2. Polymer solution is forced through a syringe at a rate of about 0.5 ml/hr, resulting in the formation of a drop of polymer solution at the tip of the needle. A high voltage (5 to 15 kV) is applied to the syringe, causing the surface of the drop to distort into the shape of a cone, as depicted in Figure 1. When a critical voltage is exceeded (typically 5 kV for the solutions discussed in this report), a jet of solution erupts from the apex of the cone and is accelerated toward the electrically grounded collection target by the macroscopic electric field (see Figure 2). As this jet travels through the air, the solvent evaporates, leaving behind a polymer fiber to be collected on an electrically grounded target. Figure 3 is an image of the electro-spinning process obtained through high-speed photography. The image clearly depicts the random motion of the electro-spinning jet as it travels toward the target. Baumgarten [9] first depicted the chaotic nature of the electro-spinning jet motion by using high speed photography. Recent work by Reneker et al. [10] suggests that this chaotic motion, or "bending instability," results (at least in part) from repulsive forces originating from the charged elements within the electro-spinning jet. Because of the chaotic motion of the electro-spinning jet as it travels to its target, deposition of electro-spun fibers on a stationary target is essentially random. This is perfectly acceptable for membrane and filter applications, which take advantage of the small pore size obtained by the random morphology of the non-woven electro-spun mat.

Collecting electro-spun fibers in the form of a yarn or "tow" (i.e., bundle of fibers) for post-processing to improve mechanical performance or depositing of electro-spun fibers on a substrate in specific places or patterns is problematic because of the random nature of the fiber deposition. Some efforts to improve control of the electro-spinning jet and deposition process include the use of both

mechanical and electrostatic means. It has been shown that electro-spun fibers can be collected in a textile where the fibers will be more or less oriented parallel to the direction of rotation [11] if the target is a drum rotating at high revolutions per minute. However, the area coated with electro-spun fibers is still quite large. It has also been shown that electro-spun fibers retain a significant portion of their charge upon deposition [2,12], and during the appropriate conditions [12], it is possible to have electro-spun fibers deposit preferentially on an aluminum screen forming a three-dimensional grid structure.

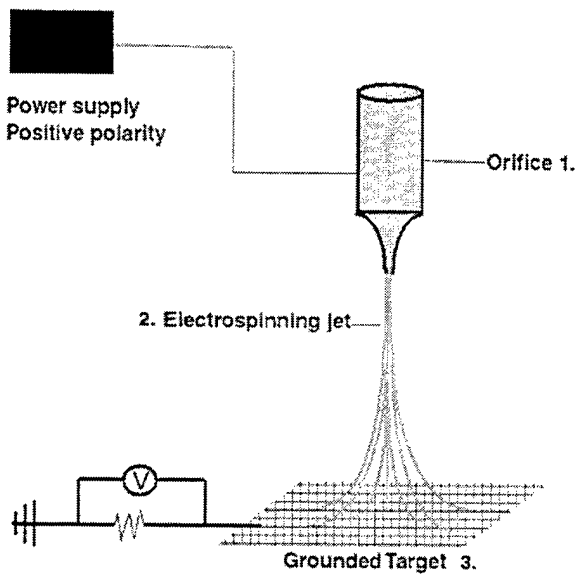

Figure 1. Standard Electro-spinning Apparatus.

Finally, Jaeger et al. [13] have demonstrated that it is possible to stop the precession of the electro-spinning jet about the tip of the syringe, which contributes to the chaotic motion of the electro-spinning jet. They accomplished this by using a single charged ring of like voltage and polarity placed concentrically about the syringe needle. Although this method of electro-spinning has the effect of stabilizing the jet at the point of initiation, the jet still undergoes bending instability as it proceeds toward the ground plane after passing through this single electrode region.

The objective of the current research has been to construct a novel electro-spinning apparatus that uses electrostatic fields (other than the one responsible for jet initiation) to dampen the bending instability inherent in the electro-spinning process. This apparatus has allowed for much greater control of the deposition and collection of electro-spun fibers. Wide angle X-ray diffraction (WAXD) analysis has been performed on electro-spun poly(ethylene oxide) (PEO) yarns collected by this apparatus, which indicated the presence of some

molecular orientation and a poorly developed crystalline microstructure within the electro-spun fibers.

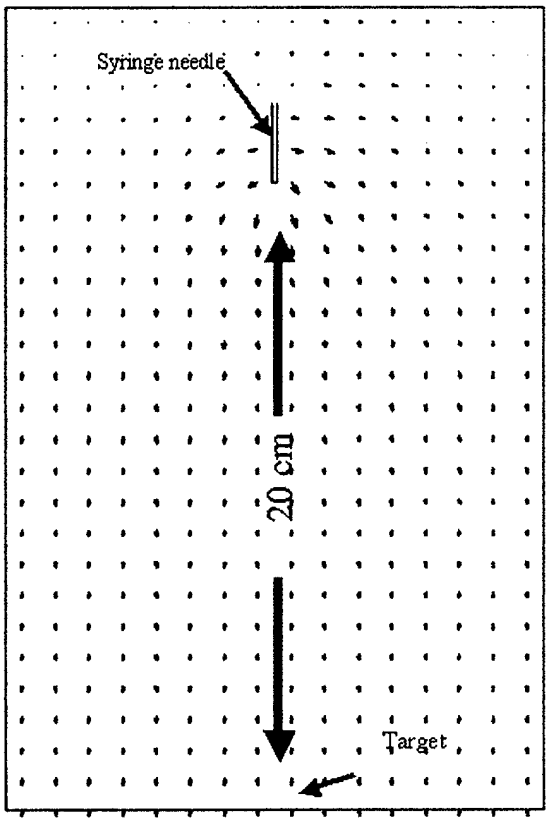

Figure 2. Field Lines Calculated for a Syringe and Grounded Target Geometry.

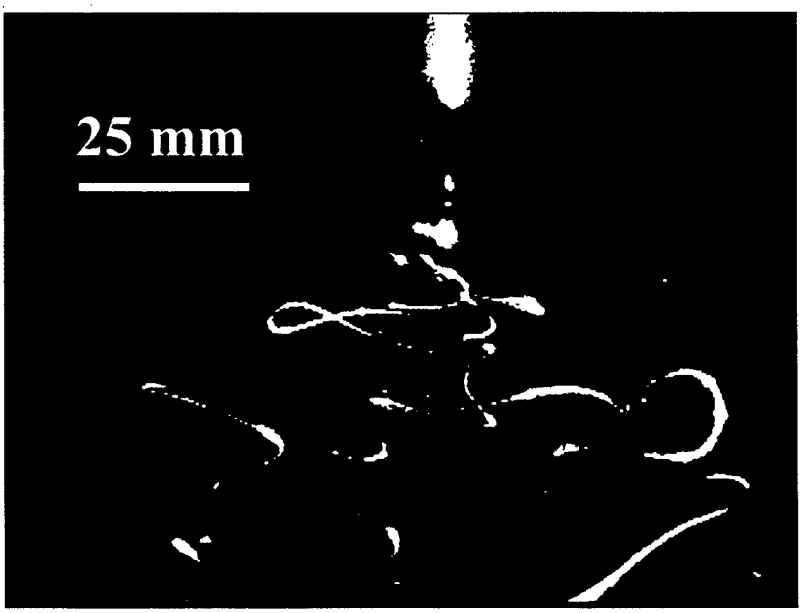

Figure 3. High Speed Image of Electro-spinning Process.

2. Experimental

PEO fibers were electro-spun from a 10% (wt) concentration of PEO in water. PEO of 400,000 molecular weight was used in making the solution. Two ES30P power supplies of positive polarity from Gamma High Voltage, Inc., were used to apply voltages of +5 to +15 kV to the vertically oriented syringe tip and rings. A Glassman Series EH high voltage power supply of negative polarity was used to apply a voltage of –9 to –12 kV to the collection plate situated at the bottom of the apparatus. Polymer solution was fed to the syringe needle tip through a Teflon® tube with a 0.125-inch inner diameter via a Harvard 2000 syringe pump. Representations of electric field lines associated with specific electro-spinning apparatus were calculated with the computer program, Student's Quick Field™. Electron micrographs of the electro-spun fibers were obtained with a Phillips Electroscan environmental scanning electron microscope.

High speed images were taken with a Photometrics cooled charge coupled device camera with a 3- by 2-k chip. The camera was attached to a Questar Schmidt-Cassegrain telescope in order to achieve high magnification from a distance of 40 cm. The electro-spinning jet was illuminated from behind with a Continuum Surelite II yttrium-aluminum-garnet laser. The laser emitted light at a wavelength of 532 nm, with a pulse duration of 10 ns. Optical micrographs of collected fibers were obtained with a Wild Makroscope M420 stereo-microscope.

Yarns of electro-spun fibers used in WAXD experiments were collected by "combing." This process involved passing two wooden splints spaced approximately 2.0 cm apart repeatedly through the electro-spinning jet about 2 cm above the collection target. WAXD analysis was performed with a Rigaku UltraX 18-kW rotating anode X-ray source and a Bruker Hi-Star 2D area detector.

3. Theory

When an external electric field is applied to a polymer solution, ions in the solution will aggregate around the electrode of opposite polarity. Positive ions travel to the negatively charged electrode and negative ions travel toward the positive electrode. This results in an excess of charge of opposite polarity in the volume of solution near an electrode. Consider a drop of polymer solution suspended at the tip of a metal syringe. When a voltage is applied to the metal syringe, the ions in the solution of like polarity will be forced to aggregate at the surface of the drop. The electric field generated by the surface charge will cause the drop to distort into the shape of a cone **[14]**. If the electric potential of the surface charge exceeds a critical value **[14]**, the electrostatic forces will overcome

the solution surface tension. A thin jet of solution will erupt from the surface of the cone and travel toward the nearest electrode of opposite polarity or electrical ground. Although the details of charge motion in the electro-spinning jet are not well understood, it is believed that excess charge is essentially static with respect the moving coordinate system of the jet [10]. This means that the electro-spinning jet can be thought of as string of charge elements connected by a visco-elastic medium, with one end fixed at the point of origin and the other end free.

As discussed in the introduction, the free end of the electro-spinning jet follows a chaotic path as it travels toward the grounded collection plate, as seen in Figure 3. This chaotic motion, or instability, is the result of a complicated interaction of variables that include viscosity, surface tension, electrostatic forces, air friction, and gravity. Recent work by Reneker et al. [10] has attempted to create a model of jet motion that takes these variables into account. This effort has met with limited success, although detailed understanding of the jet motion remains elusive. For the present discussion, it is appropriate to focus on the electrostatic forces acting on the charged elements composing the jet and the visco-elastic response of the polymer solution to these electrostatic forces.

In their work, Reneker et al. [10] proposed the following mechanism for the onset of jet instability. Upon initiation, the jet of polymer solution is rapidly accelerated away from the syringe toward the grounded target by electrostatic forces. This has the effect of providing a longitudinal stress that stabilizes the jet, keeping it initially straight. At some distance from the point of initiation, the jet of polymer solution begins undergoing stress relaxation. The point along the jet where this occurs depends on the spinning voltage, which is proportional to the strength of the macroscopic electric field [10]. By increasing the voltage, the electric field strength increases the length of the stable jet [9]. Once stress relaxation occurs, Reneker et al. [10] proposed that electrostatic interaction between the charged elements of the jet begins to dominate the ensuing motion, initiating and perpetuating the chaotic motion of the jet. This initiation of the bending instability was described in the following manner.

If one considers three unconnected point charges of equal value in a line (see Figure 4), it can be seen that the center charge, B, is acted upon by two forces of equal magnitude and opposite direction given by the equation,

$$F = kq_aq_b/r^2 = kq_cq_b/r^2 \qquad 1.$$

in which q_a, q_b , and q_c are charges of equal sign and magnitude, r is the separation between charges, and k is Coulomb's constant. Should a perturbation cause q_b to move out of line, there is a net lateral force on q_b, the magnitude of which is given by the equation

$$F_l = 2F\cos\theta \qquad 2.$$

in which θ is the angle that is formed by **r** and line perpendicular to jet axis.

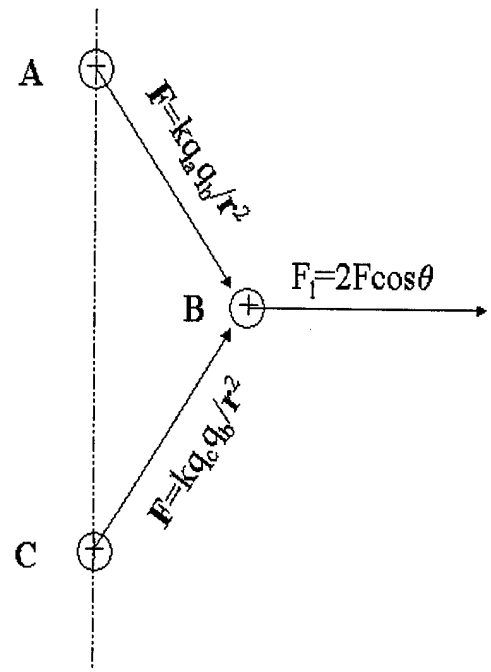

Figure 4. Forces Exerted on a Charge Element by Neighboring Charge Elements.

This lateral force, F_l, leads to an inherent instability predicted by Earnshaw's theorem **[15]**. Since an electrostatically driven jet can be thought of as a line of charged elements, it is thought that the instability predicted by Earnshaw is responsible for the onset of the chaotic motion of the free end of the electro-spinning jet **[10]**. Because any force, either electrostatic or mechanical in nature, to counter F_l is absent, the initially small perturbations grow unfettered, leading to the large looping motions that are commonly observed **[2,9,10]**.

4. Results and Discussion

It is clear from the discussion in the previous section that electrostatic interactions between individual charge elements in the jet and between charge elements and the macroscopic electric field are primarily responsible for initiation and perpetuation of the bending instability. With this knowledge, it should be possible to design an electro-spinning apparatus that can dampen or eliminate the bending instability through control of the shape and strength of the macroscopic electric field that exists as a result of the potential difference

between the point of jet initiation and the collection target (see Figures 5 and 6). The electro-spinning apparatus discussed here is similar to one first described by Melcher and Warren [16], who were studying capillary instability and jet disintegration in electrostatically driven jets of low molecular weight fluids.

The apparatus depicted in Figure 5 is different from the setup illustrated in Figures 1 and 2 in two ways. The first innovation is a series of charged rings used as an electrostatic "lens" element that changes the shape of the macroscopic electric field from the point of jet initiation to the collection target. The field lines converge to a center line above the collection target. When the charged jet passes through this field, it is forced to the center in a manner that is analogous to a stream of water that is poured into a funnel. The second difference is that the collection target has a potential bias whose polarity is opposite that of the lens element and syringe. This allows for a continuous increase in the electric field strength and a corresponding increase in downward force on the jet as it approaches the collection target (i.e., Force = q*E in which E is the field strength and q is the magnitude of the charge element in Coulombs).

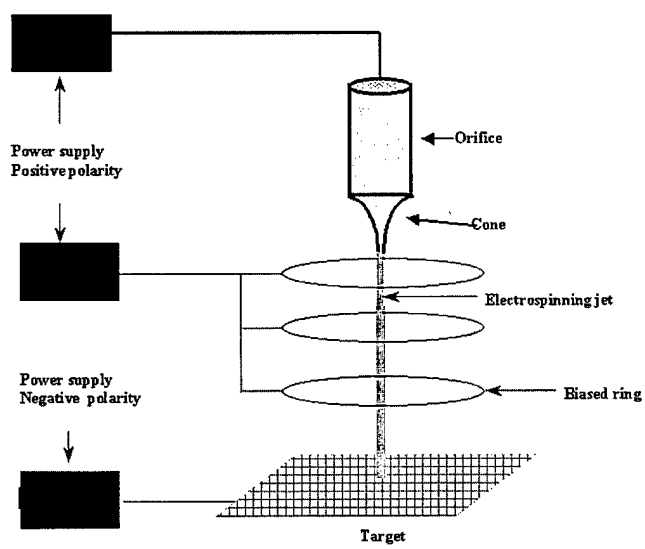

Figure 5. Multiple Field Electro-spinning Apparatus.

Figure 5 is a schematic of the multiple field electro-spinning apparatus. The apparatus consists of three high voltage power supplies. The first power supply is positive in polarity and is connected to the syringe. This is the source that supplies the critical voltage needed for jet initiation, which will be designated as the spinning voltage for the rest of this discussion. The second power supply provides the voltage for eight copper rings that are connected in series. It also provides positive polarity which will be referred to as the ring voltage. The third power supply is connected to the collection target and it provides negative polarity that will be referred to as the target voltage. The rings are 10 cm in diameter and are spaced at 1.9-cm intervals, approximately. The total distance

from the tip of the syringe to the collection target is about 20 cm. Values of +9 kV for the spinning voltage, +4 to +5 kV for the ring voltage, and 11 kV for the target voltage were usual for a typical experiment.

Figure 6 is a diagram depicting the macroscopic electric field generated by the apparatus described previously. The arrows indicate the direction of the electric field lines. The electric field is nearly uniform in direction down the center of the apparatus. At the top of the apparatus, there is a tendency for the field lines near the edge of the initiating electrode to point to the rings, which are at a lower potential. About 8 cm from the initiating electrode, the field lines start to converge at the center of the apparatus, indicating a net restoring force that acts on the charge jet. The field strength and corresponding restoring force increase as the jet approaches the target. Upon starting, there is some jet instability near the initiating electrode because of the edge effects. As the jet proceeds toward the target, the instability is dampened under the influence the converging electric field lines. Since the jet is continuous, the dampening of the instability and acceleration of the jet down stream act to stabilize the part of the jet near the initiating electrode.

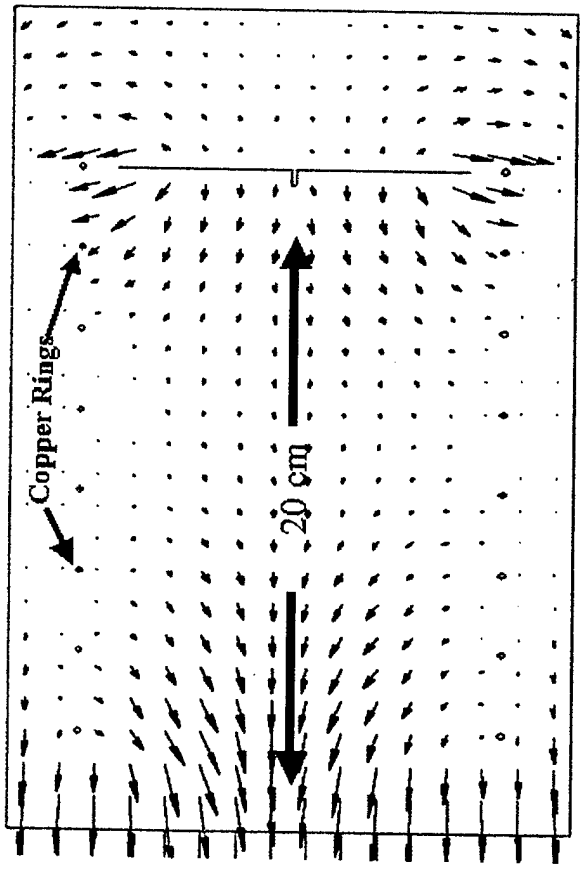

Figure 6. Field Lines Calculated for Multiple Field Electro-spinning Geometry.

Figures 7a and 7b are high-speed images of the electro-spinning jet generated with a 7% concentration solution of PEO in water with the apparatus described previously. These images were obtained about 10 cm below the syringe tip (half way to the target), which is well into the region where the bending instability normally occurs (see Figure 3). Figure 7a is an image of a straight jet with no evidence of any bending instability; Figure 7b illustrates the effect of decreasing the ring voltage from +5 kV to about +2.5 kV. In this case, the jet assumes the shape of a tight corkscrew as a result of relaxing the constraining electric field provided by the rings. When the ring voltage is increased again to 5 kV, the jet straightens.

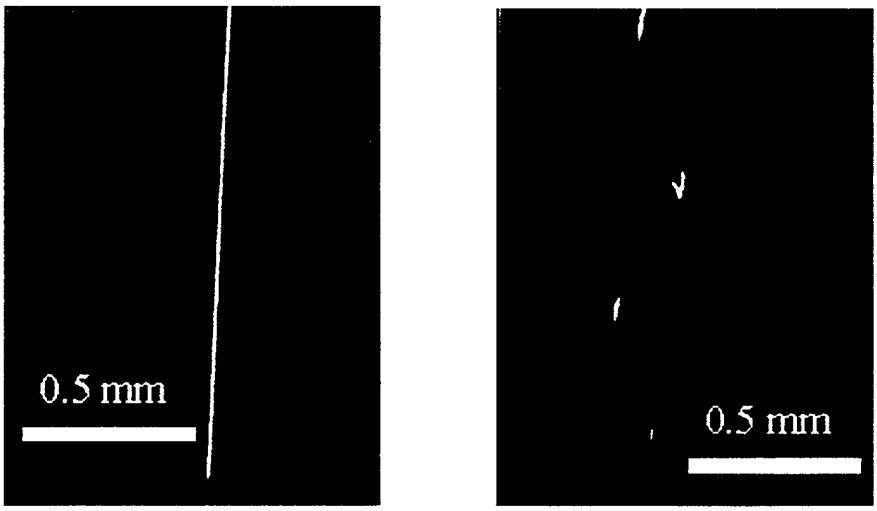

a. Ring Electrode Potential 2.5 kV b. Ring Electrode Potential 5 kV

Figure 7. Image of Electro-spinning Jet 4 inches Below Capillary Orifice.

Figures 8a and 8b are images of fiber mats electro-spun from a 10% concentration of PEO in water. Figure 8a was produced with the standard electro-spinning method, without biased lens elements. The distance from tip to target was 17 cm and the spinning voltage was about +7 kV at the syringe tip, and the fibers were collected on an aluminum screen that was electrically grounded. The fiber mat in Figure 8b was obtained with the multiple field electro-spinning apparatus via positively biased rings orifice and a negatively biased foil collection target. Comparison of these two shows the significant decrease in the diameter (from ~7 cm in 8a to ~1 cm in 8b) of the area of coverage achieved with the multiple field electro-spinning apparatus.

This reduction in the area of coverage is the result of dampening the bending instability. The multiple field technique can also affect the size of the individual fibers. Figure 9 is an electron micrograph of fibers electro-spun from 10% PEO in water with the multiple field technique. The average diameter of the fibers is 270 nm, which compares to an average diameter of 400 nm reported for PEO

electro-spun from a 10% solution with the standard method of electro-spinning, which consisted of a positively biased syringe tip (7 kV), a grounded collection target, and a tip to target distance of about 17 cm **[2]**. It is thought that the reduction in the fiber diameter is attributable to the overall change in potential from syringe tip to target being much greater for the multiple field apparatus (21 kV) used to collect the sample in the figure **[8,9]**. The fibers in Figure 9 are uniform in their overall morphology and lack beads or junctions, which indicates that most of the solvent has evaporated by the time the fibers are collected on the target.

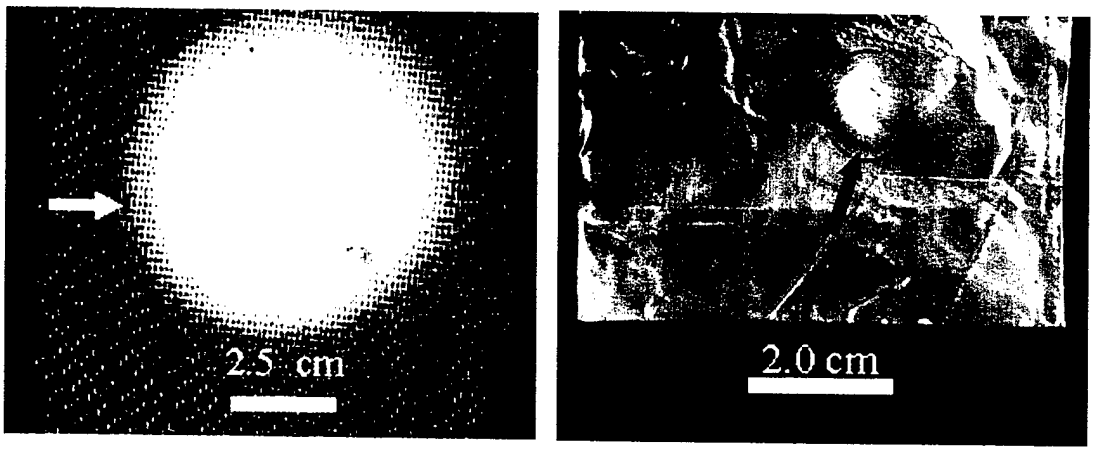

a. Standard Electro-spinning Technique Collected on Wire Mesh (diameter ~7 cm).

b. Multiple Field Technique Collected on Copper Foil (diameter ~1 cm).

Figure 8. Fibers Electro-spun From 10% Solution Concentration of PEO in Water (arrows indicate area of target covered by electro-spun fibers).

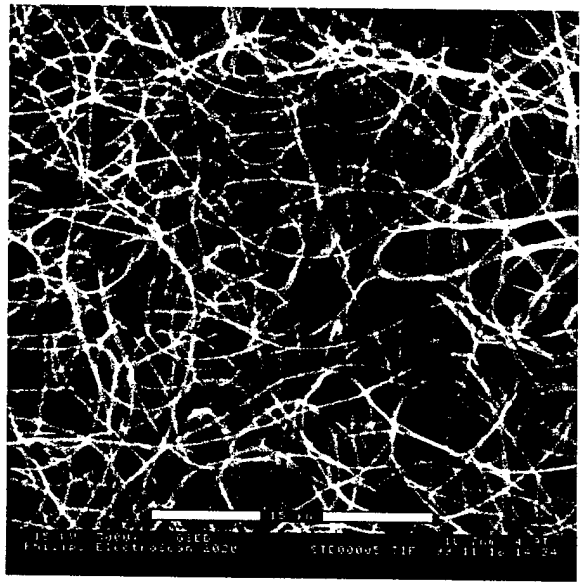

Figure 9. Electron Micrograph of PEO Fibers Electro-spun With Multiple Field Method. (Fibers were electro-spun from 10% solution concentration of PEO in water.)

When the chaotic motion of the jet is dampened, it becomes possible to deposit electro-spun fibers on a substrate in a more targeted fashion. When the target is a rotating drum covered with copper foil and charged to a potential of –11 kV, the electro-spun fibers are collected in a strip that is approximately 0.6 cm wide. Figure 10 shows two such strips collected within 0.6 cm of each other. Upon starting, some slight adjustment of the spinning voltage, ring voltage, and the solution feed rate are required in order to optimize the control of the deposition process. The strip on the right side of the image was collected during this optimization process and is slightly less well defined. After 1.5 hours, the drum was shifted slightly to the right and the second well-defined strip was collected during optimized conditions. The collection time for each strip was 1.5 hours.

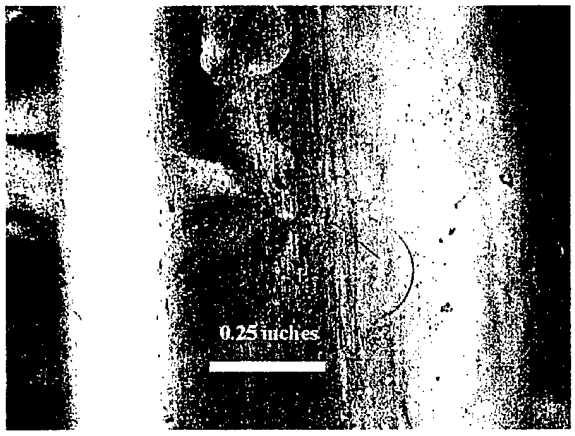

Figure 10. Electro-spun Fibers Collected on a Rotating Drum With the Multiple Field Electro-spinning Method.

It is also possible to collect electro-spun fibers in the form of a yarn with the multiple field apparatus. This was accomplished by a combing technique, in which two wooden splints spaced about 1 inch apart were repeatedly passed between the last ring and the collection plate, through the electro-spinning stream. This process allows for the collection of fibers that are more or less macroscopically oriented parallel to the direction of the combing. After 1 hour, enough electro-spun material was collected for the purpose of WAXD analysis. The fibers were removed from the splints and gently twisted into the yarns seen in Figure 11a. Figure 11b is the WAXD pattern obtained for the PEO yarns depicted in Figure 11a. The pattern shows six diffraction arcs that are characteristic of the monoclinic crystal structure of PEO. The two equatorial reflections correspond to the 120 crystallographic planes, and the four arcs in the quadrants correspond to the 112 planes. The particularly intense ring that occurs at $2\theta = 28.44°$ corresponds to the 111 reflections of the silicon powder standard.

Figure 12 is a plot of the integrated intensity of the 2D WAXD pattern in Figure 11b as a function of 2θ. When this figure is compared to a powder WAXD diffraction pattern of PEO (see Figure 13), it can be seen that the 120 and 112

reflections of the fiber pattern are relatively broad and weak with respect to the background. In addition, the powder WAXD pattern of the PEO also contains numerous higher order reflections that are not present in the fiber pattern. The broad, weak nature of the fiber pattern reflections, together with the lack of higher order reflections, indicates that the crystalline microstructure of the electro-spun fibers is not well developed. The fact that the fiber pattern reflections (see Figure 11b) show distinct arcs rather than isotropic circles like those reported for electro-spun polyethylene by Larrondo et al. [17] suggests that some degree of molecular orientation results from this multiple field electro-spinning process. Note that no attempts were made to improve the overall crystallinity or the crystal orientation through post-process, although it may be possible to improve the degree of order in the multiple field-spun fibers with standard techniques, such as annealing under tension.

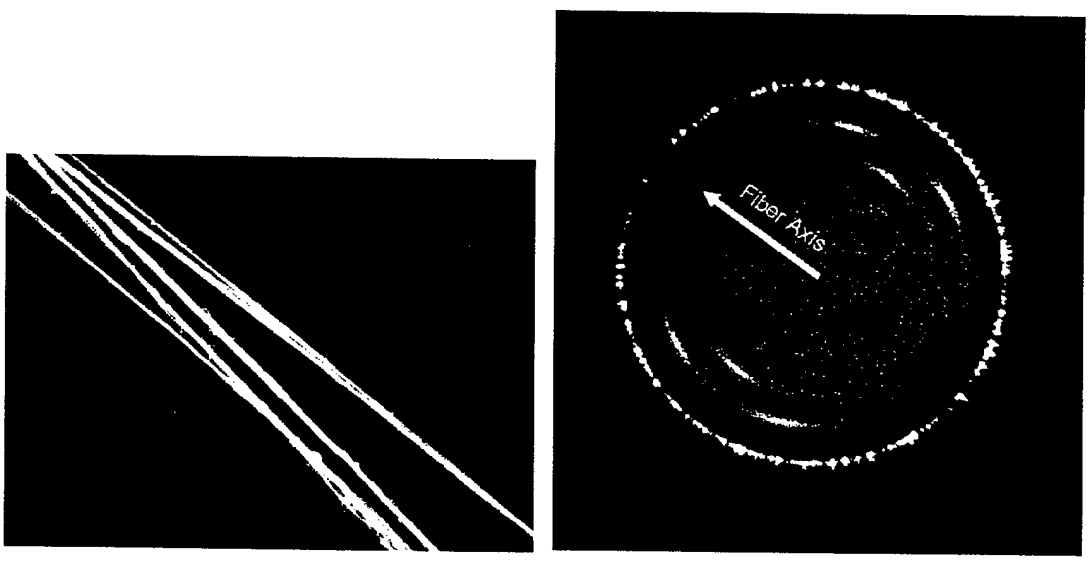

a. b.

Figure 11. 2D WAXD Pattern Obtained From PEO Electro-spun Yarns.

5. Conclusion

It has been demonstrated that it is possible to control the deposition of electro-spun fibers through the use of an electrostatic lens element and biased collection target. By the application of a secondary external field of the same polarity as the surface charge on the jet, it is possible to control or eliminate the bending instability inherent in conventional electro-spinning experiments. This mechanism allows for greater control of the deposition of electro-spun fiber on a surface and for collection of electro-spun fibers in other forms besides non-woven mats. Analyses of yarns of electro-spun polyethylene oxide via WAXD

techniques indicate the presence of some molecular orientation and a poorly developed crystalline microstructure in the fibers.

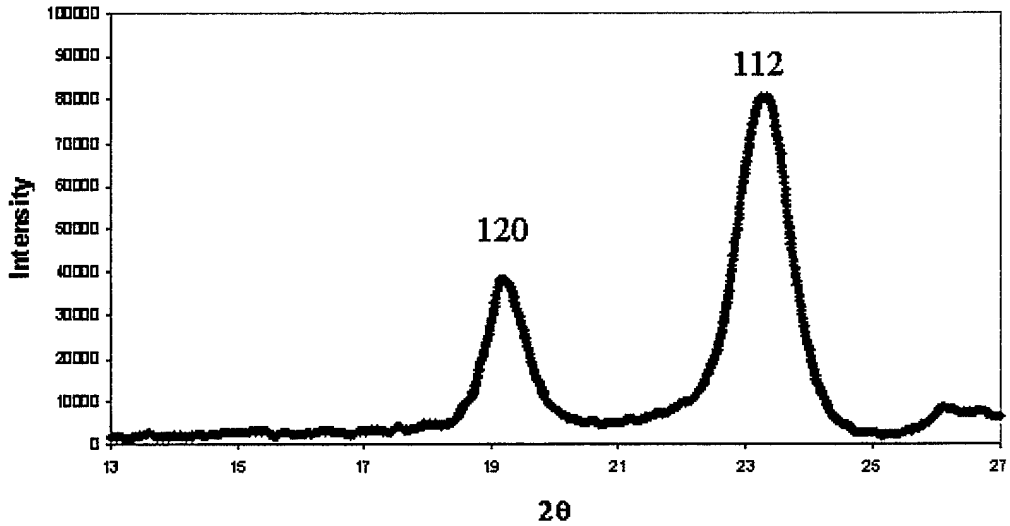

Figure 12. Plot of the Integrated Scattering Intensity as a Function of 2θ From Figure 11b.

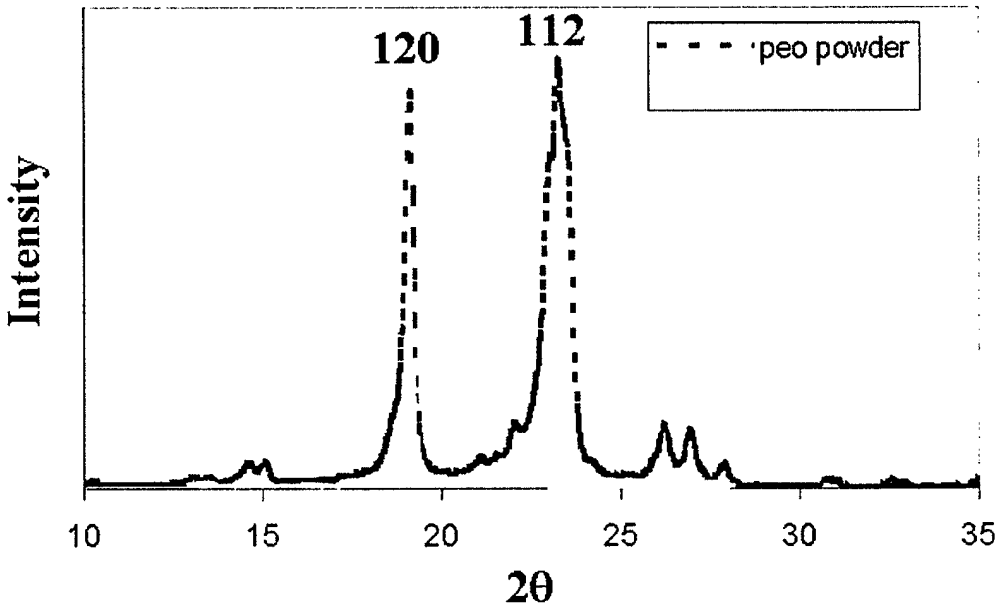

Figure 13. Powder WAXD Pattern for PEO Powder.

INTENTIONALLY LEFT BLANK

References

1. Zeleny, J., "The Electrical Discharge From Liquid Points, and a Hydrostatic Method of Measuring the Electric Intensity at Their Surfaces," Physical Review, Vol. 3, pp. 69-91, 1914.

2. Deitzel, J.M., J.D. Kleinmeyer, D. Harris, and N.C. Beck Tan, "The Effect of Processing Parameters on the Morphology of Electrospun Nanofibers and Textiles," Polymer, Issue 1, Vol. 42, pp. 261-272, 2001.

3. Reneker, D.H., and I. Chun, "Nanometer Diameter Fibres of Polymer, Produced by Electrospinning," Nanotechnology, Vol. 7, pp. 216-223, 1996.

4. Gibson, P.W., and H.L. Shreuder-Gibson, "Aerosol Particle Filtration, Gas Flow, and Vapor Diffusion Properties of Electrospun Nanofiber Coatings," Technical Report Natick/TR-99/016L XA-ASBCC, U.S. Army Soldier and Biological Chemical Command, Natick, MA, 1999.

5. Gibson, P.W., H.L. Shreuder-Gibson, and D. Rivin, "Electrospun Fiber Mats: Transport Properties," AICHE Journal, Vol. 45, pp. 190-194, 1999.

6. Buchko, C.J., L.C. Chen, Y. Shen, and D.C. Martin, "Processing and Microstructural Characterization of Porous Biocompatible Protein Polymer Thin Films," Polymer, Vol. 40, pp. 7397-7407, 1999.

7. Norris, I.D., M.M. Shaker, F.K. Ko, and A.G. MacDiarmid, "Electrostatic Fabrication of Ultra-Fine Conducting Fibers: Polyaniline/Polyethylene Oxide Blends," Synthetic Metals, Vol. 114, pp. 109-114, 2000.

8. Burgshoef, M.M., and G.J. Vancso, "Transparent Nanocomposites With Ultra-Thin Electrospun Nylon 4,6 Fiber Reinforcement," Advanced Materials, Vol. 11, No. 16, pp. 1362-1365, 1999.

9. Baumgarten, P.K., "Electrostatic Spinning of Acrylic Microfibers," Journal of Colloid and Interface Science, Vol. 36, p. 71, 1971.

10. Reneker, D.H., A.L. Yarin, H. Fong, and S. Koombhongse, "Bending Instability of Electrically Charged Liquid Jets of Polymer Solution in Electrospinning," Journal of Applied Physics, Vol. 87, pp. 4531–4547, 2000.

11. Doshi, J., and D.H. Reneker, "Electrospinning Process and Applications of Electrospun Fibers," Journal of Electrostatics, Vol. 35, pp. 151-16, 1995.

12. Deitzel, J.M., N.C. Beck Tan, J.D. Kleinmeyer, J. Rehrmann, D. Tevault, D.H. Reneker, I. Sendijarevic, and A. McHugh, "Generation of Polymer Nanofibers Through Electro-spinning," Technical Report ARL-TR-1989, U.S. Army Research Laboratory, Aberdeen Proving Ground, MD, 1999.

13. Jaeger, R., M. Bergschoof, I. Martini, C. Batelle, H. Schonherr, and G.J. Vancso, "Electrospinning of Ultra-Thin Polymer Fibers," Macromolecular Symposium, Vol. 127, pp. 141-150, 1998.

14. Taylor, G.I., "Disintegration of Water Drops in Electric Fields," Proceedings of the Royal Society of London, Series A, Vol. 280, pp. 383-397, 1964.

15. Jeans, J., "The Mathematical Theory of Electricity and Magnetism," Cambridge University Press, Cambridge, England, 1958.

16. Melcher, J.R., and E.P. Warren, "Electrohydrodynamics of a Current-Carrying Semi-Insulating Jet," Journal of Fluid Mechanics, Vol. 47, pp. 127-143, 1971.

17. Larrondo, L., and R. St. John Manley, "Electrostatic Fiber Spinning From Polymer Melts I. Experimental Observations on Fiber Formation and Properties," Journal of Polymer Science: Polymer Physics Edition, Vol. 19, pp. 909-920, 1981.

NO. OF COPIES	ORGANIZATION
1	ADMINISTRATOR DEFENSE TECHNICAL INFO CTR ATTN DTIC OCA 8725 JOHN J KINGMAN RD STE 0944 FT BELVOIR VA 22060-6218
1	DIRECTOR US ARMY RSCH LABORATORY ATTN AMSRL CI AI R REC MGMT 2800 POWDER MILL RD ADELPHI MD 20783-1197
1	DIRECTOR US ARMY RSCH LABORATORY ATTN AMSRL CI LL TECH LIB 2800 POWDER MILL RD ADELPHI MD 20783-1197
1	DIRECTOR US ARMY RSCH LABORATORY ATTN AMSRL D D SMITH 2800 POWDER MILL RD ADELPHI MD 20783-1197
1	US ARMY NRDEC ATTN SSCNC YM H GIBSON NATICK MA 01760-5020
3	US ARMY RD&E CTR ATTN P CUNNIFF D RIVIN T TASSINARI NATICK MA 01760-5020
1	PROF DAVE MARTIN 2541 CHEMISTRY BLDG 930 N UNIVERSITY AVE ANN ARBOR MI 48109-1055
1	PROF BEN HSIAO CHEMISTRY DEPT STATE UNIV OF NY AT STONY BROOK STONY BROOK NY 11794-3400
1	PROF GREG RUTLEDGE DEPT OF CHEMICAL ENG MASS INST OF TECHNOLOGY CAMBRIDGE MA 02139-4307

NO. OF COPIES	ORGANIZATION
1	LOS ALAMOS NATL LAB ATTN MS G755 CST 4 DE QUAN LI PO BOX 1663 LOS ALAMOS NM 87545
1	VA COMMONWEALTH UNIV SCHOOL OF ENGINEERING ATTN GARY E WNEK 601 W MAIN ST RM 403 P O BOX 843028 RICHMOND VA 23284-3028
1	NIST ATTN POLYMERS RSCH C GUTTMAN BLDG 224 GAITHERSBURG MD 20899
1	US ARMY SOLDIER SYSTEMS CMD US ARMY NATICK RD&E CENTER ATTN SSCNC IP QUOC TRUONG KANSAS ST NATICK MA 01760-5019
1	UNIV OF CONNECTICUT CHEMICAL ENGINEERING DEPT ATTN JEFF KOBERSTEIN 191 AUDITORIUM RD U 222 STORRS CT 06269-3222
1	DEPT OF CHEMICAL ENGINEERING UNIV OF IL AT URBANA-CHAMPAIGN ATTN ROGER ADAMS LAB MC 712 PROF TONY MCHUGH 600 S MATHEWS AVE URBANA IL 61801-3792
1	JOHN GASSNER FOSTER MILLER 103 BEAR HILL RD WALTHAM MA 02154-1196
1	UNIV OF NC AT CHAPEL HILL UNC CHEMISTRY DEPT ATTN JOE DESIMONE 211 VENABLE HALL CB #3290 CHAPEL HILL NC 27599-3290

NO. OF COPIES	ORGANIZATION
1	GOODYEAR INST OF POLYMER SCI THE UNIV OF AKRON ATTN DARRELL RENEKER AKRON OH 44325-3909
1	UNIV OF AL AT BIRMINGHAM DEPT OF CHEMISTRY ADJUNCT BIOMEDICAL & MATERIALS ENGINEERING ASST PROF R C ADVINCULA 901 S 14TH ST CHEMISTRY BLDG BIRMINGHAM AL 35294-1240
1	W L GORE & ASSOCIATES ATTN NORA BECK TAN 501 VIEVE'S WAY PO BOX 1320 ELKTON MD 21922-1320
	ABERDEEN PROVING GROUND
2	DIRECTOR US ARMY RSCH LABORATORY ATTN AMSRL CI LP (TECH LIB) BLDG 305 APG AA
50	DIRECTOR US ARMY RSCH LABORATORY ATTN AMSRL WM MA J DEITZEL BLDG 4600
1	DIRECTOR US ARMY RSCH LABORATORY ATTN AMSRL WM M G HAGNAUER BLDG 4600
1	US ARMY CBDCOM EDGEWOOD RD&E CTR ATTN D TEVAULT APG MD 21010-5423
1	US ARMY CBDCOM ATTN JEFF HALE 5232 FLEMING RD APG MD 21010-5423
	ABSTRACT ONLY
1	DIRECTOR US ARMY RSCH LABORATORY ATTN AMSRL CI AP TECH PUB BR 2800 POWDER MILL RD ADELPHI MD 20783-1197

REPORT DOCUMENTATION PAGE

Form Approved
OMB No. 0704-0188

Public reporting burden for this collection of information is estimated to average 1 hour per response, including the time for reviewing instructions, searching existing data sources, gathering and maintaining the data needed, and completing and reviewing the collection of information. Send comments regarding this burden estimate or any other aspect of this collection of information, including suggestions for reducing this burden, to Washington Headquarters Services, Directorate for Information Operations and Reports, 1215 Jefferson Davis Highway, Suite 1204, Arlington, VA 22202-4302, and to the Office of Management and Budget, Paperwork Reduction Project (0704-0188), Washington, DC 20503.

1. AGENCY USE ONLY *(Leave blank)*	2. REPORT DATE	3. REPORT TYPE AND DATES COVERED
	March 2001	Final

4. TITLE AND SUBTITLE	5. FUNDING NUMBERS
Controlled Deposition and Collection of Electro-spun Poly(ethylene oxide) Fibers	PR: 622105-AH84
6. AUTHOR(S)	
Deitzel, J.M.; Hirvonen, J.K.; Beck Tan, N.C. (all of ARL); Kleinmeyer, J.D. (XioTech)	
7. PERFORMING ORGANIZATION NAME(S) AND ADDRESS(ES)	8. PERFORMING ORGANIZATION REPORT NUMBER
U.S. Army Research Laboratory Weapons & Materials Research Directorate Aberdeen Proving Ground, MD 21005-5066	
9. SPONSORING/MONITORING AGENCY NAME(S) AND ADDRESS(ES)	10. SPONSORING/MONITORING AGENCY REPORT NUMBER
U.S. Army Research Laboratory Weapons & Materials Research Directorate Aberdeen Proving Ground, MD 21005-5066	ARL-TR-2415

11. SUPPLEMENTARY NOTES

12a. DISTRIBUTION/AVAILABILITY STATEMENT	12b. DISTRIBUTION CODE
Approved for public release; distribution is unlimited.	

13. ABSTRACT *(Maximum 200 words)*

Electro-spinning is a process by which sub-micron polymer fibers can be produced with an electrostatically driven jet of polymer solution (or polymer melt). Electro-spun fibers are typically collected in the form of non-woven mats, which are of interest for a variety of applications, including semi-permeable membranes, filters, composite reinforcement, and scaffolding used in tissue engineering. A characteristic feature of the electro-spinning process is the onset of a chaotic oscillation of the electro-spinning jet. The current work demonstrates the feasibility of dampening this instability and controlling the deposition of sub-micron polymer fibers (<300 nm in diameter) on a substrate through use of an electrostatic lens element and collection target of opposite polarity. Real-time observations of the electro-spinning process have been made with high speed, high magnification imaging techniques. Fiber mats and yarns electro-spun from polyethylene oxide have been analyzed by wide angle electron diffraction optical microscopy and environmental electron microscopy.

14. SUBJECT TERMS	15. NUMBER OF PAGES
electro-spinning nano-fibers	25
	16. PRICE CODE

17. SECURITY CLASSIFICATION OF REPORT	18. SECURITY CLASSIFICATION OF THIS PAGE	19. SECURITY CLASSIFICATION OF ABSTRACT	20. LIMITATION OF ABSTRACT
Unclassified	Unclassified	Unclassified	

NSN 7540-01-280-5500

Standard Form 298 (Rev. 2-89)
Prescribed by ANSI Std. Z39-18
298-102